Protonation effects on the resonance Raman properties of a novel (terpyridine)Ru(*4H*-imidazole) complex: An experimental and theoretical case study

Stephan Kupfer[1], Julien Guthmuller[1], Maria Wächtler[1,2,3], Sebastian Losse[4], Sven Rau[5,6], Benjamin Dietzek[1,2,3], Jürgen Popp[1,2,3], Leticia González[1,2*]

[1]*Institute for Physical Chemistry, Friedrich Schiller University Jena, Helmholtzweg 4, 07743, Jena, Germany*

[2]*Abbe Center of Photonics, Friedrich Schiller University Jena*

[3]*Institute for Photonic Technology (IPHT) Jena, Albert-Einstein-Str. 9, 07745, Jena, Germany*

[4] *Leibniz-Institut für Katalyse e. V. (LIKAT) Albert-Einstein-Str. 29 a, 18059 Rostock (Germany)*

[5] *Friedrich-Alexander-University Erlangen-Nuremberg, Department of Chemistry and Pharmacy, Egerlandstrasse 1, 91058 Erlangen (Germany)*

[6] *University of Ulm, Institute of Inorganic Chemistry I, Albert-Einstein-Allee 11, 89081 Ulm (Germany)*

*leticia.gonzalez@uni-jena.de

Supplementary Information

- The RITP(H) absorption spectra and excited states calculated with the PBE0 functional in acetonitrile are presented on Fig. S1 and Table S1, respectively.
- The RITP(H) absorption spectra and excited states calculated with the CAM-B3LYP functional in acetonitrile are presented on Fig. S2 and Table S2, respectively.
- The molecular orbitals of RITP(H) calculated with PBE0 and CAM-B3LYP are presented on Table S3.
- The ^{1}H and ^{13}C NMR spectra of RITP and RITPH are presented in Fig. S3 to S6

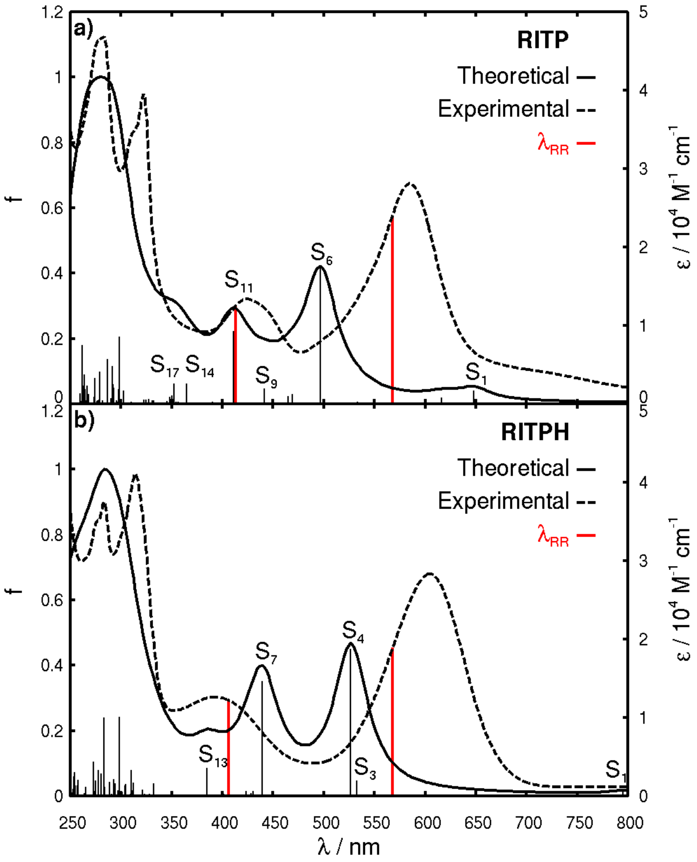

Figure S1: Experimental (dashed line) and theoretical (PBE0, black line) absorption spectra of the RITP and RITPH species in acetonitrile. The calculated oscillator strengths are represented by black sticks. A Lorentzian function with a half-width of 20 nm is employed to broaden the transitions in the simulated spectrum. The two vertical lines indicate the wavelengths at which the RR measurements are performed for the unprotonated (568 and 413 nm) and the protonated species (568 and 406 nm).

Table S1: Calculated (PBE0) vertical excitation energies (E^{e}), oscillator strengths (*f*) and singly-excited configurations of the main excited states and experimental absorption maxima in the visible range. The principal orbitals are depicted on Table S3.

State	Transition	Weight (%)	E^{e} (eV)	λ (nm)	f	λ_{Exp} (nm)
	RITP					
S_1	$d_{xz}(182) \rightarrow \pi^{*}_{im}(183)$ (MLCT)	94	1.91	648	0.040	720
S_6	$d_{xy}(181) \rightarrow \pi^{*}_{im}(183)$ (MLCT)	53	2.50	497	0.422	585
	$d_{yz}(180) \rightarrow \pi^{*}_{terpy}(184)$ (MLCT)	28				
	$d_{yz}(180) \rightarrow \pi^{*}_{im}(183)$ (MLCT)	8				
S_9	$d_{yz}(180) \rightarrow \pi^{*}_{terpy}(184)$ (MLCT)	29	2.81	441	0.046	-
	$d_{xy}(181) \rightarrow \pi^{*}_{terpy}(185)$ (MLCT)	27				
	$d_{xy}(181) \rightarrow \pi^{*}_{im}(183)$ (MLCT)	14				
	$d_{xz}(182) \rightarrow \pi^{*}_{terpy}(185)$ (MLCT)	10				
S_{11}	$\pi_{im}(179) \rightarrow \pi^{*}_{im}(183)$ (IL)	92	3.01	411	0.224	425
S_{14}	$d_{xz}(182) \rightarrow \pi^{*}_{terpy}(186)$ (MLCT)	92	3.40	365	0.062	-
S_{17}	$\pi_{im}(178) \rightarrow \pi^{*}_{im}(183)$ (IL)	53	3.52	352	0.061	-
	$d_{xz}(182) \rightarrow \pi^{*}_{terpy}(187)$ (MLCT)	32				
	RITPH					
S_1	$d_{xz}(182) \rightarrow \pi^{*}_{im}(183)$ (MLCT)	94	1.56	795	0.012	-
S_3	$d_{xz}(182) \rightarrow \pi^{*}_{terpy}(184)$ (MLCT)	91	2.33	533	0.048	-
S_4	$d_{xy}(180) \rightarrow \pi^{*}_{im}(183)$ (MLCT)	78	2.36	526	0.450	605
S_7	$\pi_{im}(179) \rightarrow \pi^{*}_{im}(183)$ (IL)	91	2.82	439	0.352	386
S_{13}	$\pi_{im}(178) \rightarrow \pi^{*}_{im}(183)$ (IL)	97	3.22	385	0.085	-

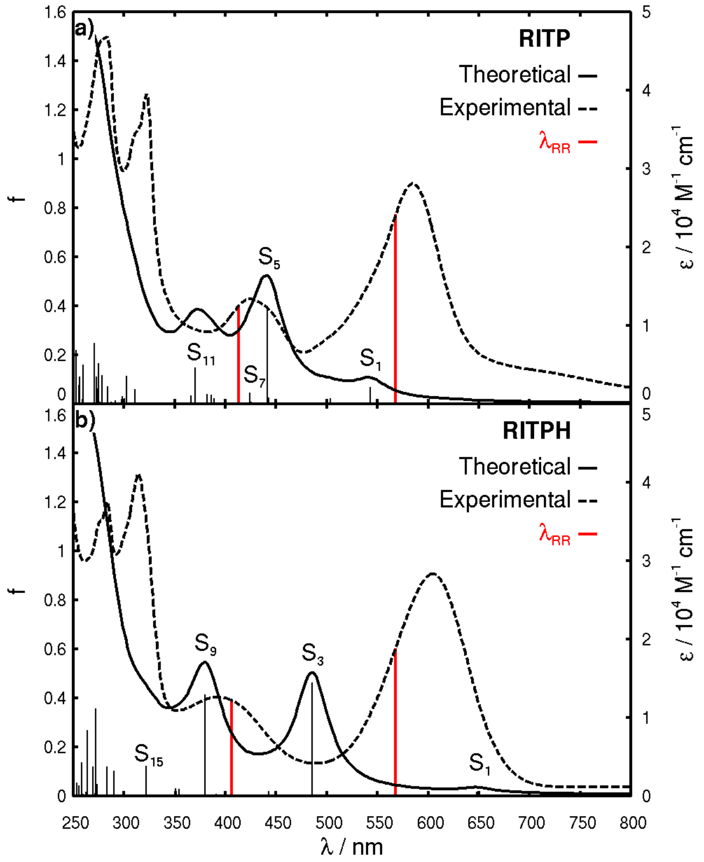

Figure S2: Experimental (dashed line) and theoretical (CAM-B3LYP, black line) absorption spectra of the RITP and RITPH species in acetonitrile. The calculated oscillator strengths are represented by black sticks. A Lorentzian function with a half-width of 20 nm is employed to broaden the transitions in the simulated spectrum. The two vertical lines indicate the wavelengths at which the RR measurements are performed for the unprotonated (568 and 413 nm) and the protonated species (568 and 406 nm).

Table S2: Calculated (CAM-B3LYP) vertical excitation energies (E^e), oscillator strengths (*f*) and singly-excited configurations of the main excited states and experimental absorption maxima in the visible range. The principal orbitals are depicted on Table S3.

State	Transition	Weight (%)	E^e (eV)	λ (nm)	*f*	λ_{Exp} (nm)
	RITP					
S_1	$d_{xz}(182) \rightarrow \pi^*_{im}(183)$ (MLCT)	89	2.28	543	0.068	720
S_5	$d_{xy}(181) \rightarrow \pi^*_{im}(183)$ (MLCT) $d_{yz}(180) \rightarrow \pi^*_{terpy}(184)$ (MLCT)	56 32	2.81	441	0.401	585
S_7	$d_{xz}(182) \rightarrow \pi^*_{terpy}(185)$ (MLCT) $d_{yz}(180) \rightarrow \pi^*_{terpy}(184)$ (MLCT) $d_{xy}(181) \rightarrow \pi^*_{im}(183)$ (MLCT)	34 26 11	2.92	424	0.046	-
S_{11}	$\pi_{im}(179) \rightarrow \pi^*_{im}(183)$ (IL) $\pi_{im}(177) \rightarrow \pi^*_{im}(183)$ (IL)	72 9	3.35	370	0.148	425
	RITPH					
S_1	$d_{xz}(182) \rightarrow \pi^*_{im}(183)$ (MLCT)	87	1.91	648	0.018	-
S_3	$d_{xy}(180) \rightarrow \pi^*_{im}(183)$ (MLCT) $d_{yz}(181) \rightarrow \pi^*_{im}(183)$ (MLCT)	69 11	2.55	485	0.464	605
S_9	$\pi_{im}(179) \rightarrow \pi^*_{im}(183)$ (IL)	84	3.26	380	0.416	386
S_{15}	$\pi_{im}(178) \rightarrow \pi^*_{im}(183)$ (IL)	88	3.86	322	0.123	-

Table S3: Molecular orbitals involved in the main configurations of the states responsible for the absorption and RR properties of the unprotonated (RITP) and protonated (RITPH) complexes.

PBE0		**CAM-B3LYP**	
RITP	**RITPH**	**RITP**	**RITPH**
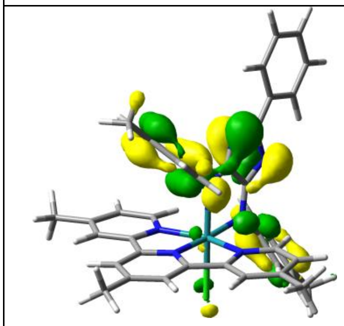 $\pi_{im}(177)$	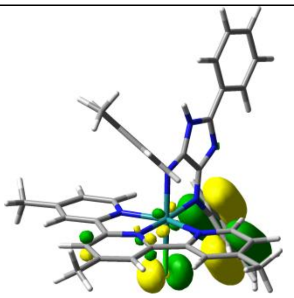 $\pi_{im}(177)$	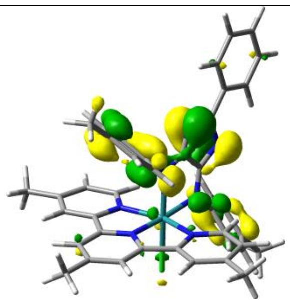 $\pi_{im}(177)$	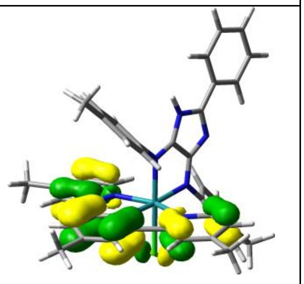 $\pi_{terpy}(177)$
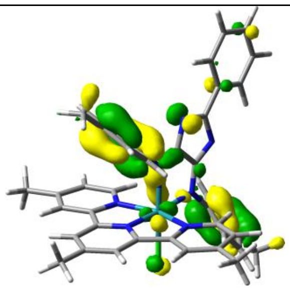 $\pi_{im}(178)$	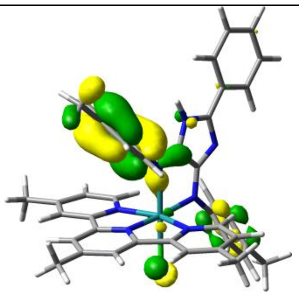 $\pi_{im}(178)$	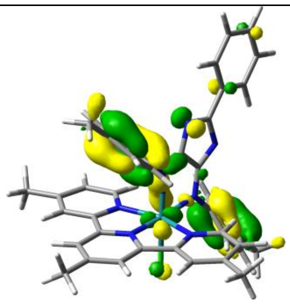 $\pi_{im}(178)$	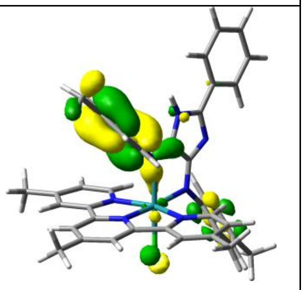 $\pi_{im}(178)$
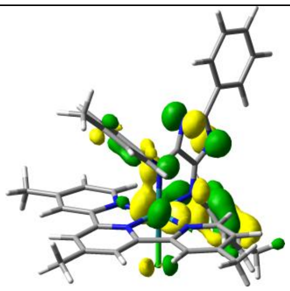 $\pi_{im}(179)$	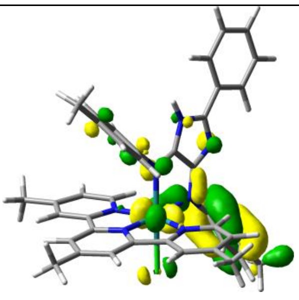 $\pi_{im}(179)$	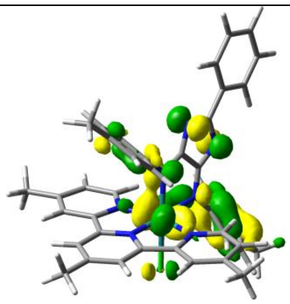 $\pi_{im}(179)$	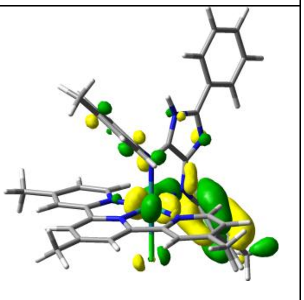 $\pi_{im}(179)$

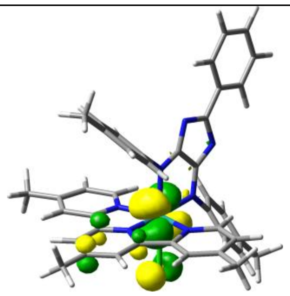 d_{yz}(180)	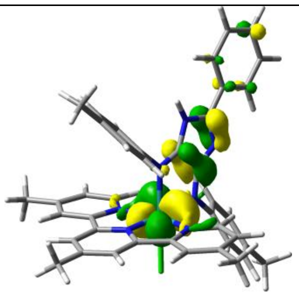 d_{xy}(180)	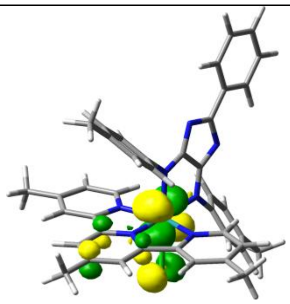 d_{yz}(180)	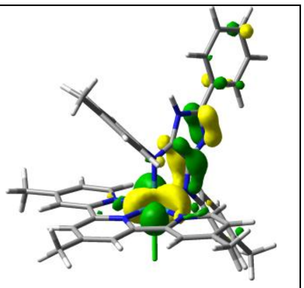 d_{xy}(180)
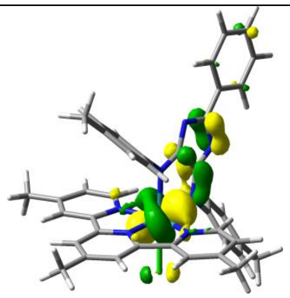 d_{xy}(181)	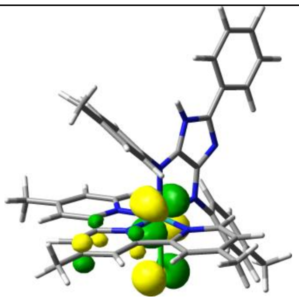 d_{yz}(181)	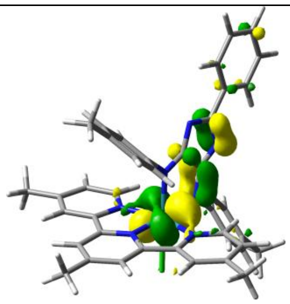 d_{xy}(181)	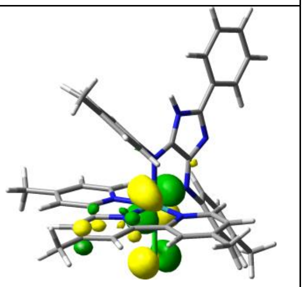 d_{yz}(181)
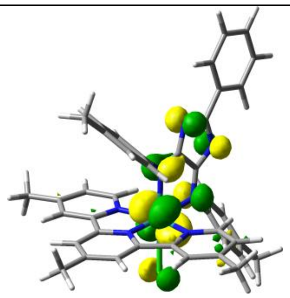 d_{xz}(182)	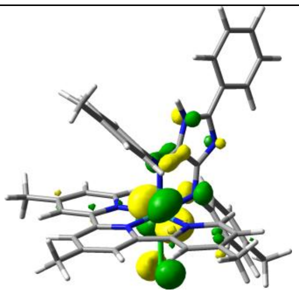 d_{xz}(182)	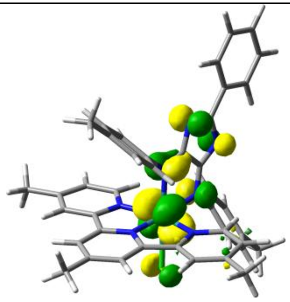 d_{xz}(182)	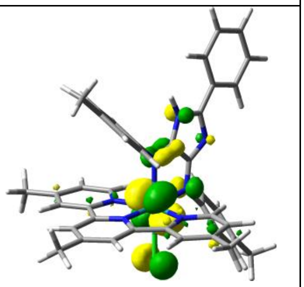 d_{xz}(182)
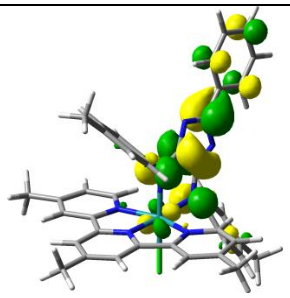 π^*_{im}(183)	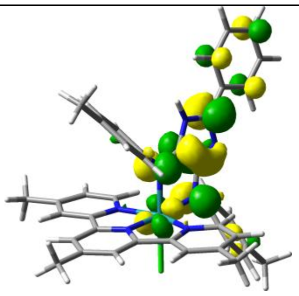 π^*_{im}(183)	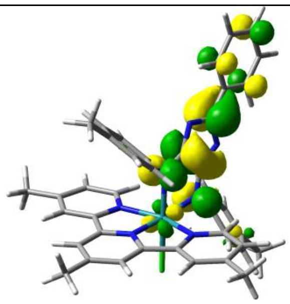 π^*_{im}(183)	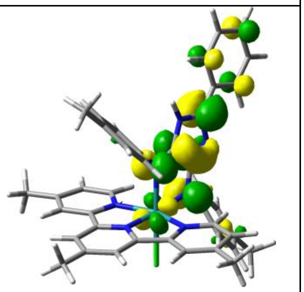 π^*_{im}(183)

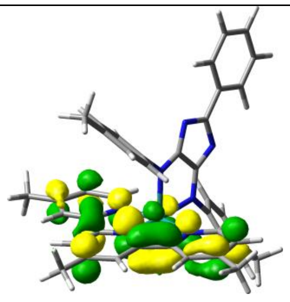 $\pi^{*}_{\mathrm{terpy}}(184)$	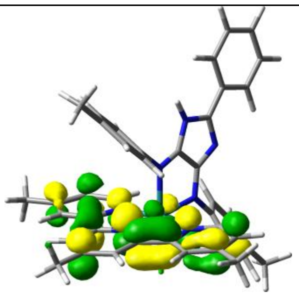 $\pi^{*}_{\mathrm{terpy}}(184)$	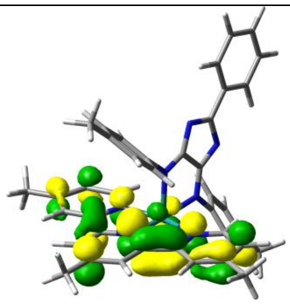 $\pi^{*}_{\mathrm{terpy}}(184)$	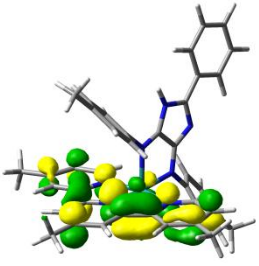 $\pi^{*}_{\mathrm{terpy}}(184)$
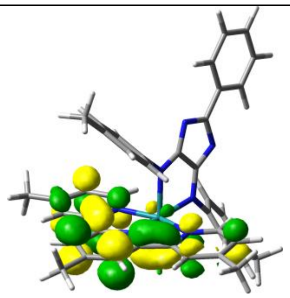 $\pi^{*}_{\mathrm{terpy}}(185)$	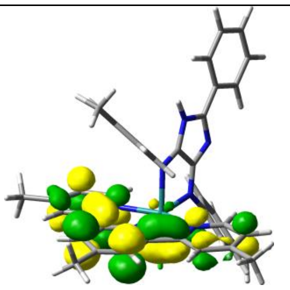 $\pi^{*}_{\mathrm{terpy}}(185)$	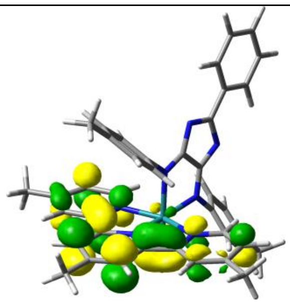 $\pi^{*}_{\mathrm{terpy}}(185)$	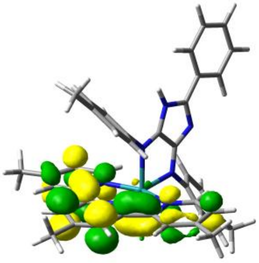 $\pi^{*}_{\mathrm{terpy}}(185)$
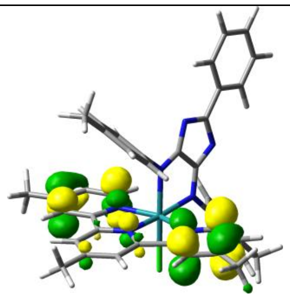 $\pi^{*}_{\mathrm{terpy}}(186)$	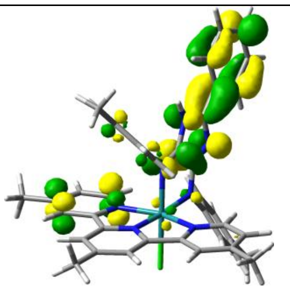 $\pi^{*}_{\mathrm{im}}(186)$	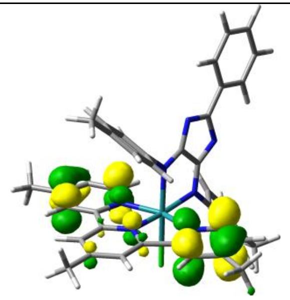 $\pi^{*}_{\mathrm{terpy}}(186)$	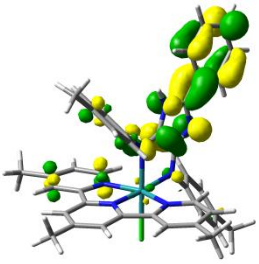 $\pi^{*}_{\mathrm{im}}(186)$
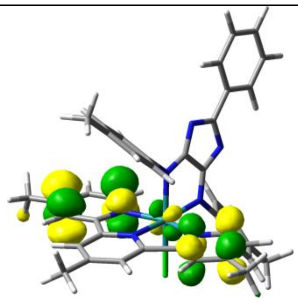 $\pi^{*}_{\mathrm{terpy}}(187)$	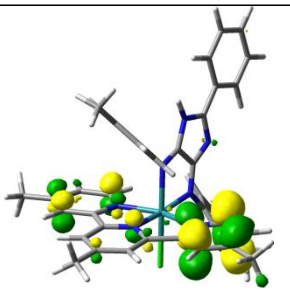 $\pi^{*}_{\mathrm{terpy}}(187)$	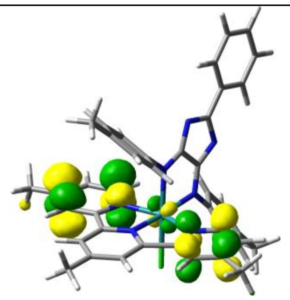 $\pi^{*}_{\mathrm{terpy}}(187)$	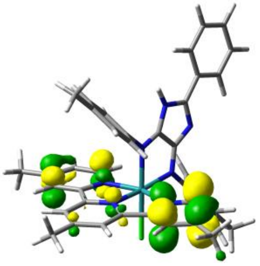 $\pi^{*}_{\mathrm{terpy}}(187)$

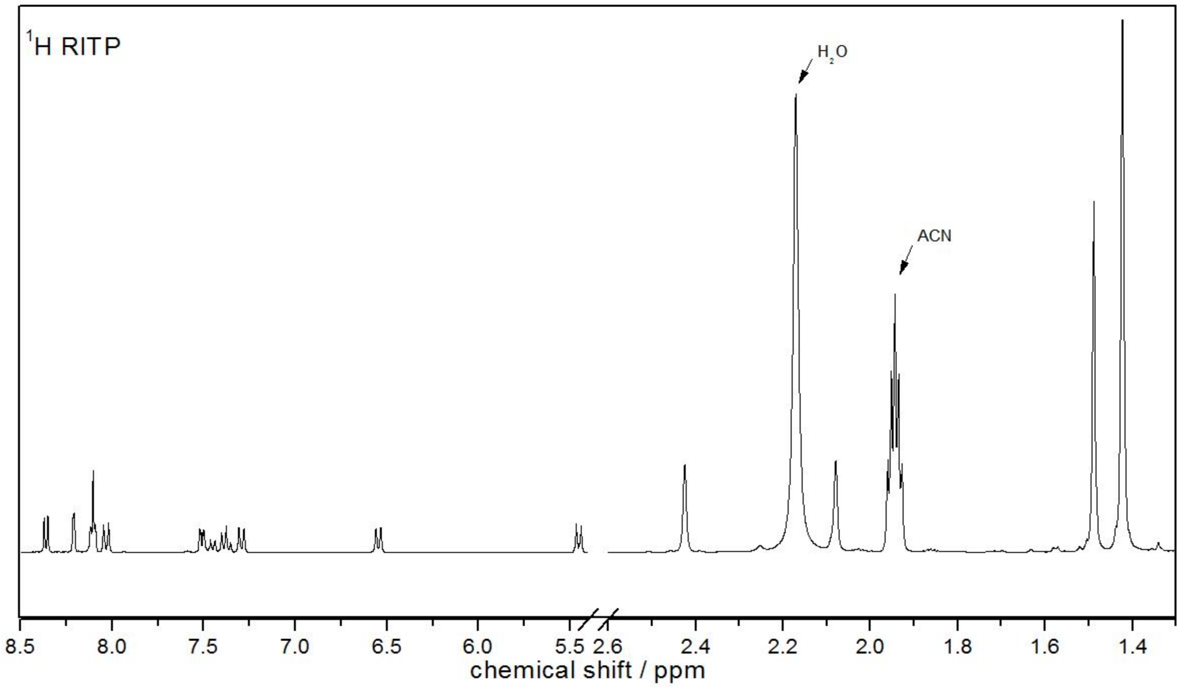

Figure S3: ^{1}H NMR spectrum of RITP

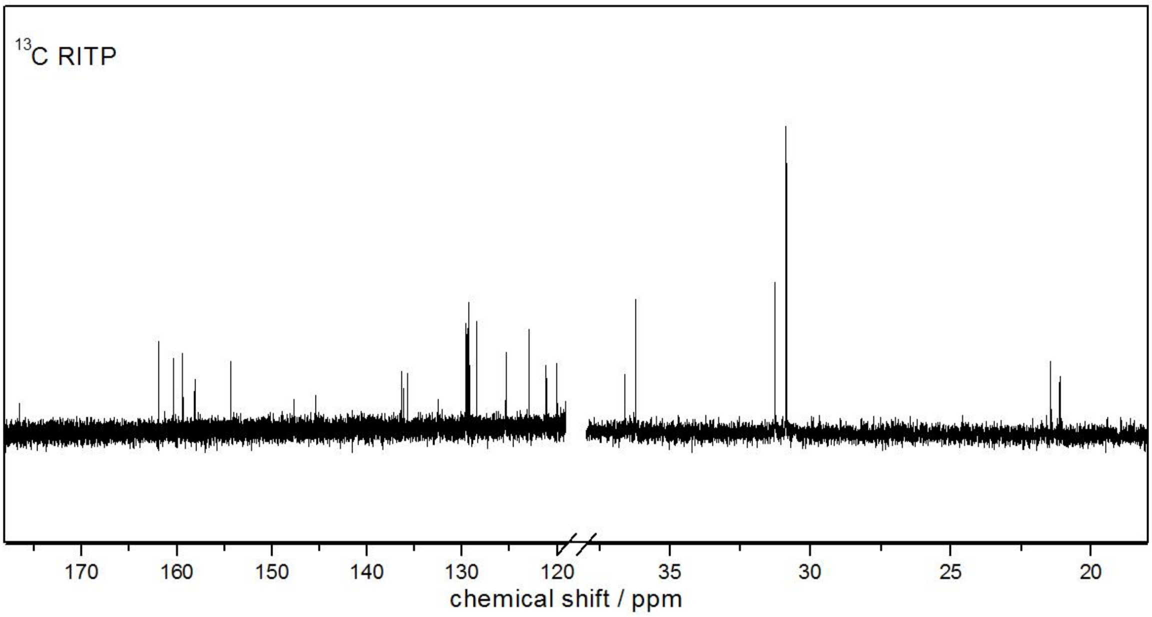

Figure S4: ^{13}C NMR spectrum of RITP

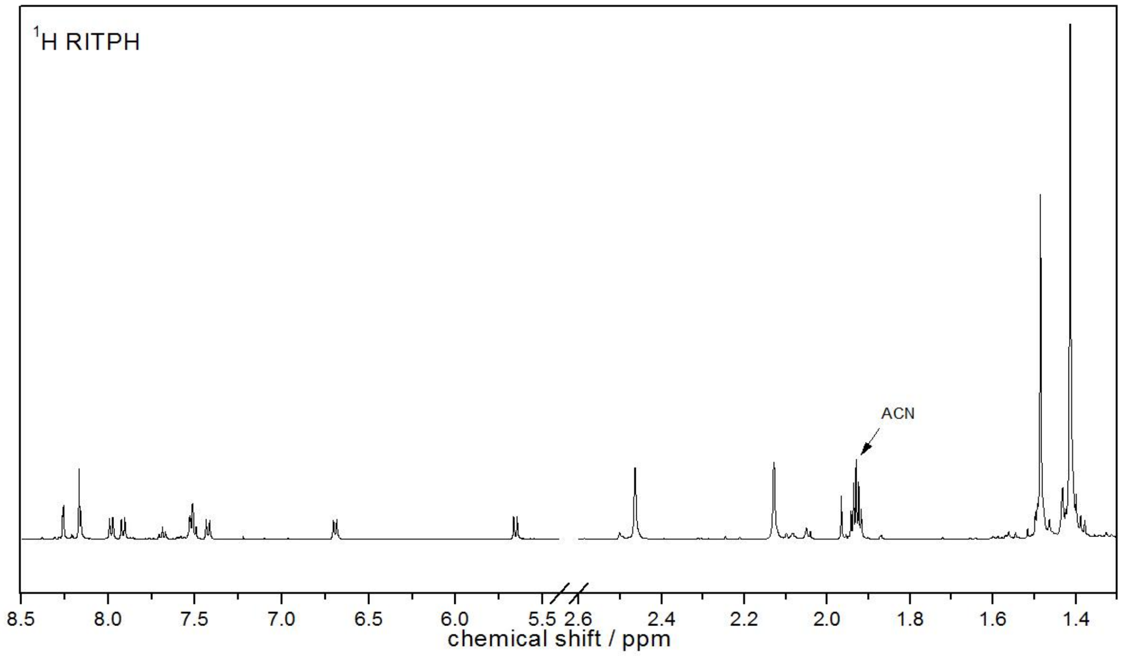

Figure S5: ^{1}H NMR spectrum of RITPH

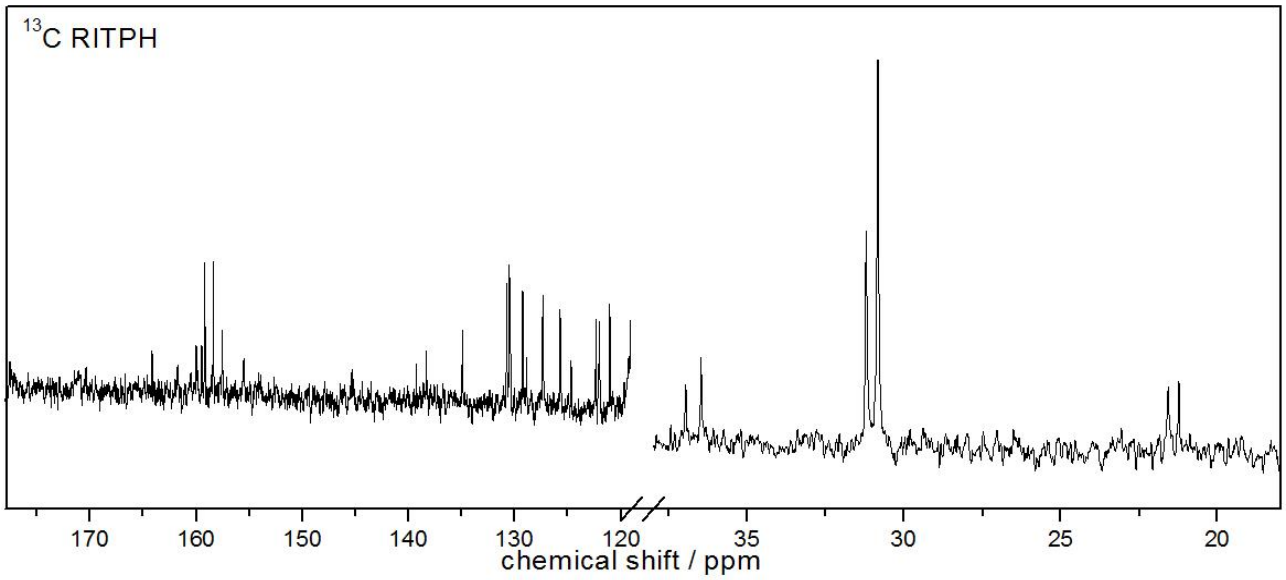

Figure S6: ^{13}C NMR spectrum of RITPH